

P. Prabukanthan¹, M. Sreedhar¹, G. Harichandran², T. Tatarchuk³, K. Dinakaran⁴,
S. Uthayakumar^{5,6} and A. Younis⁷

Physicochemical and Electrocatalytic Performance of Chromium doped Iron Pyrite Thin Films

¹Materials Chemistry Lab, Department of Chemistry, Muthurangam Government Arts College, Vellore-632002, India, pprabukanthan76@hotmail.com

²Department of Polymer Science, University of Madras, Guindy Campus, Chennai-600025, India

³Educational and Scientific Center of Materials Science and Nanotechnology, Vasyl Stefanyk Precarpathian National University, Ivano-Frankivsk, 76018, Ukraine

⁴Department of Chemistry, Thiruvalluvar University, Vellore-632115, India

⁵Department of Physics, Royal Holloway University of London, Egham, TW20 0EX, UK

⁶ISIS Facility, STFC, Rutherford Appleton Laboratory, Didcot, Oxfordshire OX11 0QX, UK

⁷Department of Physics, College of Science, University of Bahrain, Sakhir Campus, Kingdom of Bahrain

Chromium (Cr³⁺) doped iron pyrite (FeS₂) thin films were deposited on ITO substrate by a facile electrochemical deposition process. The effect of chromium content on structural, optical, electrical, morphological, and electrocatalytic behavior of the pyrite thin films were examined. X-ray diffraction studies confirmed the formation of cubic crystal structure of deposited thin films. Atomic force microscopy results indicate that Cr³⁺ doping has strong influence on crystallinity, surface roughness and grain size of as-deposited thin films. Further, bandgap reduction was found in Cr³⁺ doped FeS₂ thin films. The interfacial charge resistance of fabricated thin films was investigated by electrochemical impedance spectroscopy and 3 mole % Cr³⁺ doped FeS₂ thin films showed excellent conductivity with a low charge transfer resistance of 49 Ω. Further, the electrocatalytic performance of the prepared pyrite thin films was investigated. Cr doped thin films were found to exhibit better performance. Anti-structural modeling was opted to investigate the characteristics of defects in fabricated thin films and it was established that Cr³⁺ substitution may form cation (Fe²⁺) vacancies which could be responsible for enhanced photochemical and electrochemical activities in Cr-doped FeS₂ thin films.

Keywords: electrochemical deposition; semiconductor thin films; pyrite; impedance spectroscopy; electrocatalytic activity; surface analysis.

Received 4 October 2021; Accepted 2 February 2022.

Introduction

Recently, metal chalcogenide based semiconductors have attracted enormous research interests particularly for their applicability in optoelectronic devices. Also, the nontoxic and earth abundant nature of pyrite made them favorable for solar to electrical energy conversion and storage [1-2]. In addition, iron pyrite thin films has a superb extensive interest for energy functional materials in past decades and in particularly field of optoelectronics, and semiconductors due to its suitable

band gap energy ($E_g \approx 0.95$ eV) with high optical absorption coefficient [3-6]. Moreover, thin films of iron pyrite have diverse applicability in various electrochemical and industrial applications [7], quantum sensitized solar cells [8], optical, batteries, magnetic device and in thermoelectric applications [9-10]. Moreover, the transition metal ion doped semiconducting materials have considerable magnetic behavior and also enhanced photovoltaic optical properties and because of their environmental compatibility [11-12].

Several deposition routes were adopted to grow FeS₂ thin films such as microwave irradiation [15], metal

organic chemical vapor deposition (MOCVD) [13-14], radio frequency sputtering (RF) [17], sulfurization of iron films [16], flash evaporation [18], chemical vapor transport (CVT) [19], hydrothermal [20], solvo-thermal [21], electrochemical deposition (ECD) [22] and aerosol-assisted chemical vapor deposition [23], respectively. Among them electrochemical deposition method is considered as simple, low cost, environmental friendly and easy to control method for growing thin films. Although, there have been few studies on fabrication of FeS₂ thin films for various applications, but to the best of our knowledge, the effect of Cr doping in FeS₂ thin films have rarely been reported. In the present work, we report fabrication of Cr³⁺ doped FeS₂ thin films using a simple, cost effective and facile electrochemical deposition (ECD) approach. The influence of Cr³⁺ doping in FeS₂ thin films on structural, morphological, electrical, optical and electrochemical properties were investigated.

I. Experimental procedure

1.1. Materials used

Ferrous sulphate heptahydrate (FeSO₄·7H₂O), thiourea ((NH₂)₂CS, 99%), chromium acetate (Cr(CH₃COO)₃·xH₂O) and tin doped indium oxide (ITO) substrates were purchased from Sigma-Aldrich, India. Sulfuric acid (H₂SO₄) and Sodium sulfate (Na₂SO₄) were purchased from spectrochem, India. All of these chemicals are analytical grade and used as received.

1.2. Fabrication of Cr³⁺ doped FeS₂ thin films

The ITO glass substrate was used to electrochemically deposit thin films of FeS₂. For a typical deposition, aqueous solution containing 0.03 mol dm⁻³ of FeSO₄·7H₂O, 0.003 mol dm⁻³ of (NH₂)₂CS and various amounts (1 - 5 mole %) of Cr³⁺ ions as a source of iron, sulfur and chromium, were used. The electrochemical deposition process was carried out using linear sweep voltammetry (LSV) technique with three electrodes setup in the potential range of -1.0 V to

+1.0 V at a scan rate of 1.5 mV/S using an electrochemical workstation (CH604, CH Instrument USA). A platinum (Pt) wire was used as counter electrode, Ag⁺/AgCl (saturated KCl) electrode as reference electrode and the ITO substrate was used as working electrode. The deposition was carried out at 0.55 V for 10 minutes at 50 °C and the LSV profiles of various Cr-doped FeS₂ thin films are illustrated in Fig. 1. After the deposition, the ITO substrate was cooled to room temperature before using for any other characterizations. All the composite nanostructures deposited on the ITO substrate have a thickness in the range of 540 - 790 nm.

Characterizations

The crystallinity of the Cr³⁺ ions doped FeS₂ thin films were studied using XRD recorded in the range of 2 θ from 20 to 80 ° with Cu K_α (λ = 1.5406 nm) radiation source in a XPERT-PRO instrument. The electrocatalytic performance of FeS₂ and Cr³⁺ doped FeS₂ thin films were studied by cyclic voltammetry (CV) measurements using an electrochemical analyzer (CHI604E), CH Instruments Inc. A standard three-electrode cell was used with a Ag⁺/AgCl (in saturated KCl) as a reference electrode, Pt-wire as a counter electrode and pyrite thin films coated ITO substrate as working electrode. Transient photocurrent investigations were carried out with a 100 W Xenon lamp (OSRAM, Germany), where 0.1 M Na₂SO₄ solution was used as electrolyte. The electrochemical impedance spectroscopy (EIS) analysis on the Cr³⁺ ions doped FeS₂ thin films was carried out by AC-impedance method at AC amplitude of 5 mV at room temperature in the frequency range of 0.1 Hz to 1.0 MHz. The atomic force microscopy (AFM) NT-MDT, Ireland was used to study topography of FeS₂ and Cr³⁺ doped FeS₂ thin films. Auger electron spectroscopy (AES) was carried out on the prepared thin films in a Perkin Elmer thin film analyzer with an applied beam current of 180 nA and a modulation voltage of 5 eV peak to peak, under an UHV environment. The samples were sputter etched before analysis using a V.G. Scientific ion gun with

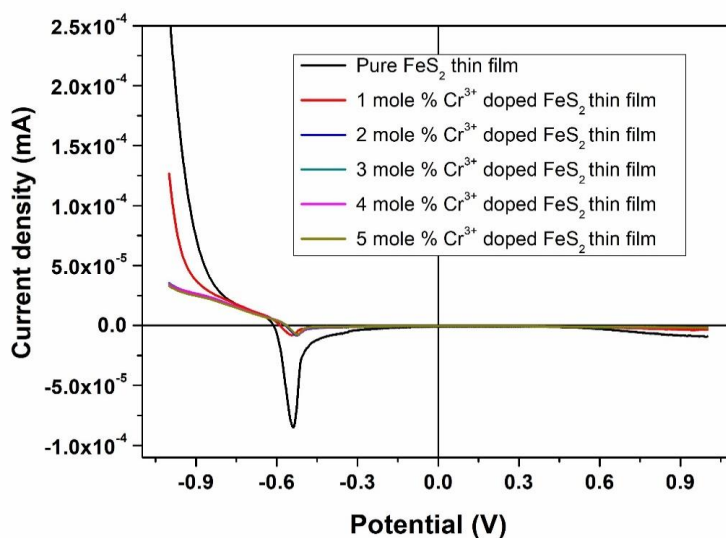


Fig. 1. LSV profile for the deposition of Cr³⁺ doped FeS₂ thin films.

3 keV Ar⁺ to remove surface contamination, at a pressure of 5.4 x 10⁻⁹ Torr during the analysis.

II. Results and discussion

2.1. X-ray diffraction (XRD) Studies

The XRD spectra of various FeS₂ and doped FeS₂ with different chromium concentrations (i.e. 1, 2, 3, 4 and 5 mole %) are shown in Fig. 2.

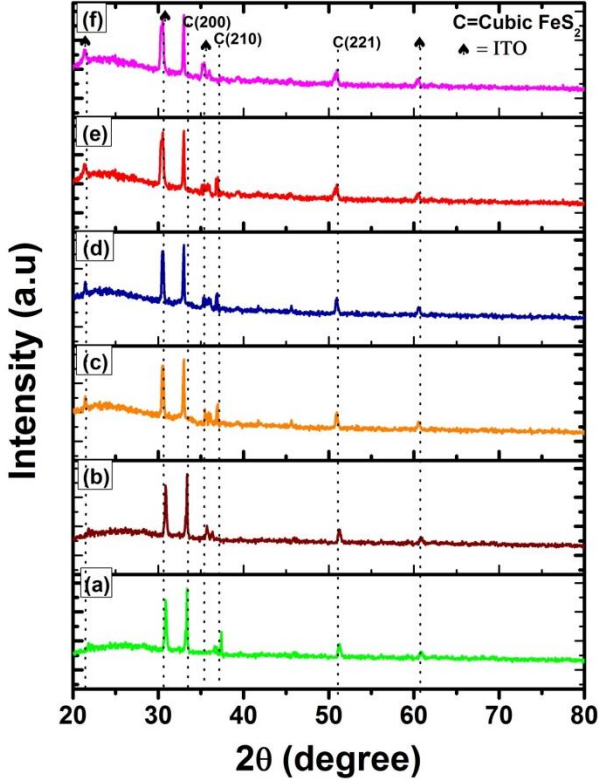


Fig. 2. XRD spectra of as-deposited (a) undoped FeS₂, (b) 1 mole %, (c) 2 mole %, (d) 3 mole %, (e) 4 mole % and (f) 5 mole % Cr³⁺ doped FeS₂ thin films.

The diffraction peaks for undoped and Cr³⁺ doped FeS₂ thin films correspond to (200), (210) and (221) cubic crystal planes of FeS₂ (JCPDS no. 42-1340). No impurity peaks were detected which indicates that Cr was successfully doped into FeS₂ matrix without any secondary phase. However, a slight shift in peak positions towards low diffracted angles was observed for doped samples which may be attributed to a slight difference in ionic radii of Cr³⁺ ions (0.63 Å) and Fe²⁺ ions (0.61 Å). By replacing Fe with slightly bigger Cr ion may produce elongation in the unit cell which slightly increase lattice parameters; hence higher d-spacing and a lower angle peak shifting can be observed [25]. Furthermore, it can be confirmed that the doping of Cr³⁺ into FeS₂ lattice does not formed any other phase formation. The lattice constants, average crystallite size and micro strains in each sample were calculated using following equations and their values are mentioned in Table-1.

$$a = d (h^2 + k^2 + l^2)^{1/2}, \quad (1)$$

where; d is inter-planar spacing in the lattice. The considered values of d -spacing are used for determination of full width half maximum. The Scherrer formula explain the average crystallite size and calculated by using full width at half maximum values of preferentially sloping diffraction peaks.

$$D = 0.9 \lambda / (\beta \cos\theta), \quad (2)$$

where; λ is the wavelength of X-ray and β is the full width half maximum of the diffraction line in radians. The calculated average crystallite sizes were found to be in the range of 92 - 107 nm as shown in Table-1. The dislocation density (δ) micro strain (ϵ), and number of crystallites per unit area (N) have been estimated through the following relations and their values are given in Table 1.

$$\text{Micro strain } (\epsilon) = \beta \cos\theta/4 \quad (3)$$

Table 1.

FWHM, crystallite size, micro strain, dislocation density, number of crystallites per unit area of undoped and Cr³⁺ doped FeS₂ thin films.

Samples	FWHM of XRD peak (200)	Lattice constants	Crystalline size (nm)	Micro strain (x10 ⁻³)	Dislocation density (x10 ²⁴ lines/m ²)	No. of crystallites per unit area (x10 ¹⁵ m ⁻²)
Undoped FeS ₂	0.1567	5.3734	92.36	3.7	0.12	0.9
1 mole % Cr ³⁺ doped FeS ₂	0.1510	5.3734	95.85	3.6	0.10	2.3
2 mole % Cr ³⁺ doped FeS ₂	0.1396	5.4728	103.70	3.34	0.92	5.3
3 mole % Cr ³⁺ doped FeS ₂	0.1382	5.4728	104.71	3.31	0.91	5.4
4 mole % Cr ³⁺ doped FeS ₂	0.1347	5.4728	107.39	3.22	0.86	5.9
5 mole % Cr ³⁺ doped FeS ₂	0.1341	5.4332	107.90	3.21	0.85	6.2

$$\text{Dislocation density } (\delta) = 15\epsilon/aD \quad (4)$$

$$\text{Number of crystallites } (N) = t/D^3 \quad (5)$$

where; t is film thickness, θ is the Bragg's angle, δ is familiar physical phenomena of thin films and ϵ is the strain which induces a deformation in 1 ppm. The breadth and roughness values of undoped and Cr³⁺-doped FeS₂ were noted through profilometry and listed in Table 2.

2.2. Optical properties

UV-visible spectroscopy was conducted to investigate the bandgap of undoped and Cr doped FeS₂ thin films and the results in the form of Tauc's relation (plotted against $(\alpha h\nu)^2$ and photon energy ($h\nu$) are

depicted in Fig. 3. Bandgaps were found to be reduced by increasing Cr doping concentration in FeS₂ and the recorded bandgap values were determined as 0.90, 0.899, 0.897, 0.896, and 0.889 eV respectively, corresponding to 1, 2, 3, 4 and 5 mole % Cr³⁺ doped-FeS₂ thin films, [26-27]. Generally, bandgaps decrease with the increase of crystallite size [28], thickness and crystalline nature [29], roughness, and grain size. Our results are consistent with the XRD data, where increased crystal size was obtained by increasing Cr doping content in FeS₂ thin films. Another possible reason of bandgap reduction by Cr doping could be due to sp-d exchange interactions between the band electrons in FeS₂ and the localized d-electrons of the Cr³⁺ ions [30-33].

2.3. Atomic Force Microscopy

The surface morphology and topography of electrochemically deposited un doped and Cr doped FeS₂

Table 2.

Thickness and roughness values of undoped and Cr³⁺ doped FeS₂ thin films.

Samples	Thickness (nm)	Roughness (nm)
Undoped FeS ₂ thin film	485	60
1 mole % Cr ³⁺ doped FeS ₂ thin film	570	84
2 mole % Cr ³⁺ doped FeS ₂ thin film	595	93
3 mole % Cr ³⁺ doped FeS ₂ thin film	628	98
4 mole % Cr ³⁺ doped FeS ₂ thin film	740	105
5 mole % Cr ³⁺ doped FeS ₂ thin film	790	110

Table-3.

Impedance data of undoped and Cr³⁺ doped FeS₂ thin films.

Samples	R_s (Ohm.cm ²)	R_b (Ohm.cm ²)	R_{ct} (Ohm.cm ²)
Undoped FeS ₂ thin film	85	4722	4637
1 mole% Cr ³⁺ doped FeS ₂	98.26	4611	4512.0
2 mole% Cr ³⁺ doped FeS ₂	390.3	662	271.7
3 mole% Cr ³⁺ doped FeS ₂	69	118	49
4 mole% Cr ³⁺ doped FeS ₂	216	529	313
5 mole% Cr ³⁺ doped FeS ₂	108	219	111

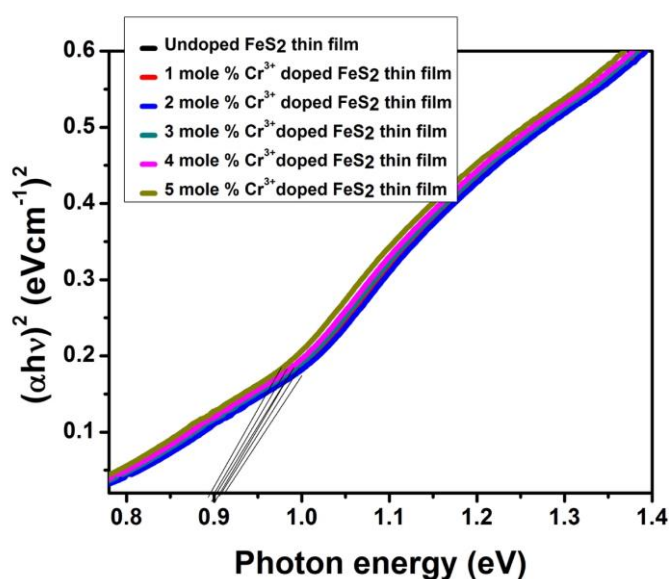


Fig. 3. Absorption coefficient vs photon energy spectra of undoped and Cr³⁺ doped FeS₂ thin films.

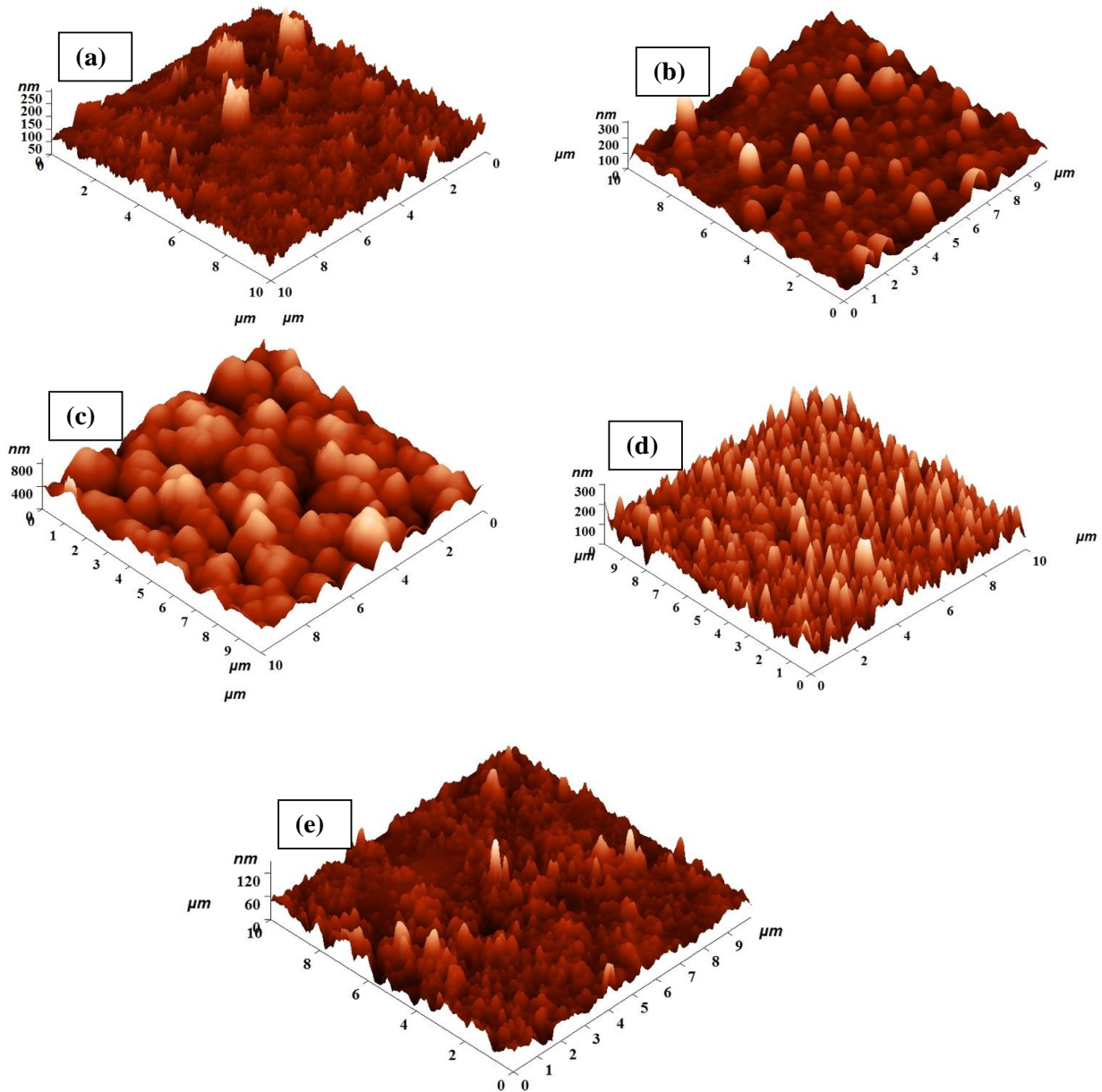


Fig. 4 (a-e). AFM images of as-deposited a) 1 mole %, (b) 2 mole %, (c) 3 mole %, (d) 4 mole % and (e) 5 mole % Cr³⁺ doped FeS₂ thin films.

thin films were investigated through atomic force microscopy (AFM) as shown in Figs. 4, (a-e). The as-prepared thin films showed good crystallinity and grains are quite visible and decently uniform in size. The average roughness (R_a) and root-mean square roughness (RMS) of all samples were recorded in the range of 48.5 - 101.67 nm and 46.31 - 128.36 nm, respectively. It is noteworthy to mention here that the roughness and RMS are slightly higher than undoped FeS₂ thin film. Furthermore, the crystal grain sizes increase with higher Cr doping which further support our XRD results. By replacing Fe ion (0.061 nm) with Cr ion (0.063 nm), a slight elongation is produced within the crystal structure, which could be a possible reason for larger crystal grain size and higher surface roughness for doped samples. [32]

2.4. Electrochemical impedance spectroscopy (EIS) analysis

The electrochemical impedance spectroscopy (EIS) was employed to examine the electrochemical properties of Cr³⁺ doped FeS₂ thin films and the results are present in Fig. 5. The charge transfer resistance (R_{ct}) which shows that 3 mole % Cr³⁺ doped FeS₂ thin film has lower value due to the smaller semicircle diameter compared to the other films. The undoped FeS₂ and other Cr³⁺ doped FeS₂ thin film has a small arc radius on the impedance plot, which is beneficial to the separation of electrons and holes. It is also noted that the lower the charge transfer resistance and faster interfacial charge transfer reaction of 3 mole % Cr³⁺ doped FeS₂ thin film can be explained for the smaller arc radius. Thus, the smaller charge transfer resistance of 3 mole % Cr³⁺ doped FeS₂ is most favorable for higher electrocatalytic activity.

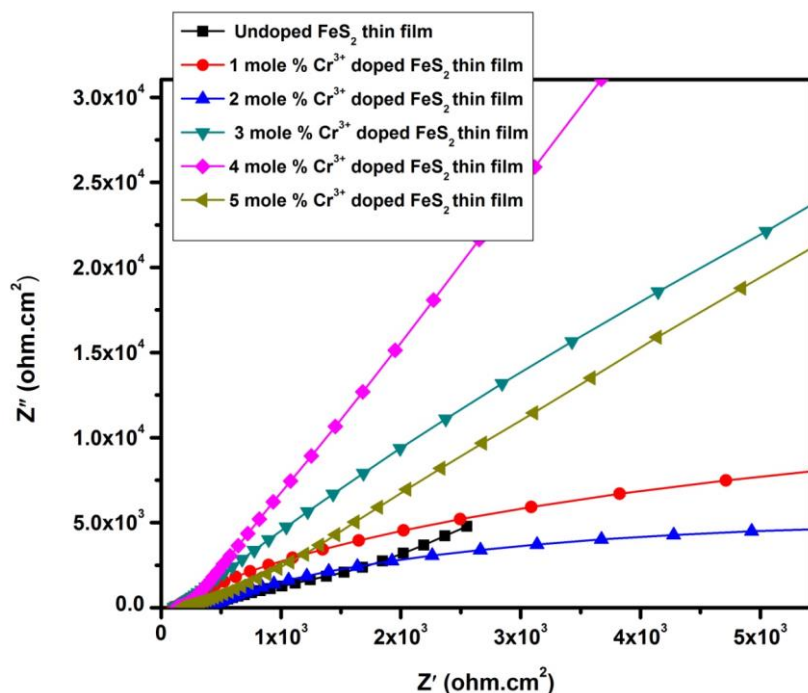


Fig. 5. Nyquist plots of undoped and Cr^{3+} doped FeS_2 thin films.

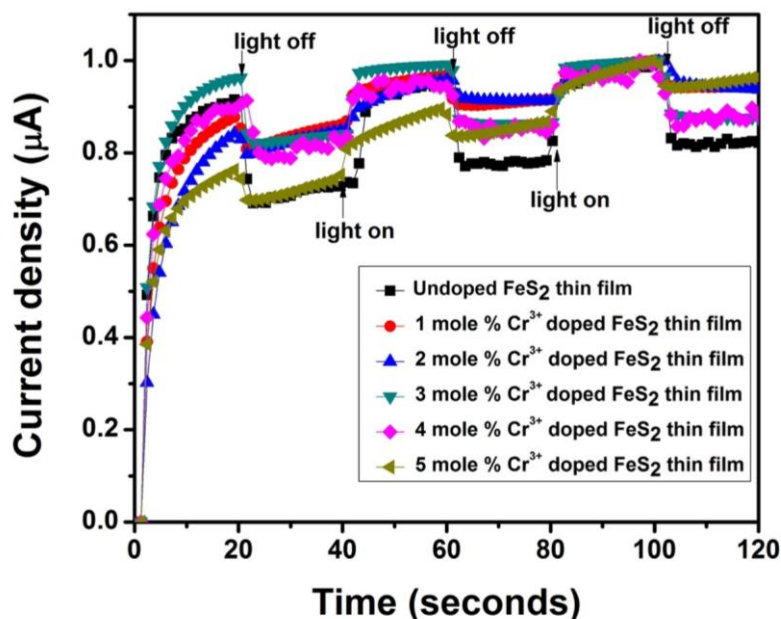


Fig. 6. Transient-photocurrent response of Nyquist plots of undoped and Cr^{3+} doped FeS_2 thin films.

2.5. Photocurrent studies

The photocurrent responses of undoped and Cr^{3+} doped FeS_2 thin films were investigated and the results are presented in Fig. 6. All samples expressed fast and uniform photocurrent responses. With the implication of UV light, an increase in current for all samples was observed due to the photo excitation of electron from valence band into conduction band. The photocurrent density of 3 mole % Cr^{3+} doped FeS_2 thin film was found as highest ($0.9841 \mu\text{Acm}^{-2}$) among all other samples. Overall, the Cr doped FeS_2 thin films demonstrated higher photocurrent response than undoped ones. A slow electron hole recombination could be one of the possible reasons for the high photocurrent of Cr^{3+} doped FeS_2 .

Moreover, the higher photocurrent densities in doped samples indicate improved conductivity of samples which is in accord to our EIS results. Chromium doping can also induce some defects in FeS_2 matrix which in turn increase the overall conductivity of doped samples [34]

2.6. Electrocatalytic activity

Cr^{3+} doped FeS_2 thin films were tested for their electro catalytic activity through cyclic voltammetry (CV) with three electrode systems as shown in Fig. 7. The results showed two pairs of redox peaks (Ox-1/Red-1, Ox-2/Red-2) in all the profiles, among them lower potential assigned to the oxidation and

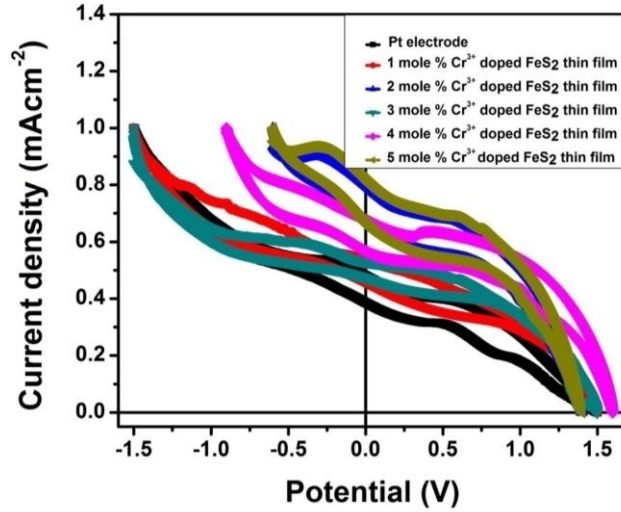


Fig. 7. The cyclic voltammogram curves of 1 to 5 mole % Cr³⁺ doped FeS₂ thin films.

reduction of iodide /tri-iodide, according to equation 6 and the redox peaks at higher potential (Ox-2 and Re-2) can be ascribed to the redox reaction shown in equation 7.

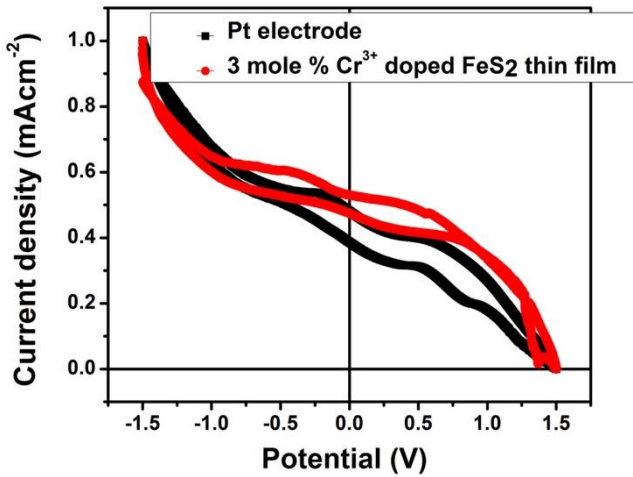


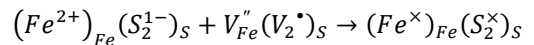
Fig. 8. The cyclic voltammogram curves of standard Pt and 3 mole % Cr³⁺ doped FeS₂ thin film at 100 mV/S scan rate.

It is observed from the cyclic voltammetry curves that all the prepared samples, 1 - 5 mole % Cr³⁺ ions doped FeS₂ thin films, has identical voltagrams as that of Pt proposing similar electro catalytic behavior for the iodide/tri-iodide redox reaction. The Ox-1 and Red-1 peaks are focus of our analysis because that could reveal the catalytic reduction of I₃⁻ to I⁻ ions. The peak-to-peak separation (EPP) and the peak current density (IPC) and are the critical parameters for comparing electrocatalytic activities of different thin film counter electrodes. A higher catalytic activity for 3 mole % Cr doped FeS₂ thin film can be inferred from higher intense reduction IPC and a lower EPP values. The cathodic and anodic peak currents of Cr³⁺ ion doped FeS₂ thin films are determined to be a little higher than that of Pt, indicating enhanced

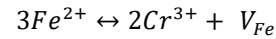
electro catalytic activity of the prepared films. Further, the smaller peak to peak separation value (ΔE_{pp}) and higher peak current density of 3 mole % Cr³⁺ doped FeS₂ thin film validated their higher catalytic performance toward the reduction of I₃⁻. As shown in the Fig. 8, the 3 mole % Cr³⁺ doped FeS₂ thin film intimately resembles the profile equivalent to the redox reactions of I₃⁻ with the Pt.

2.7. Antistructure modeling

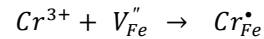
An antistructure modeling is mostly used to understand the enhanced photocatalytic activity of Cr³⁺ doped FeS₂ materials [34-36]. The information's about surface active sites and lattice defects can be obtained through the superposition of crystallo-chemical structure with FeS₂ antistructure: $V_{Fe}''(V_2^*)_S$, where • – a single positive charge; '' – a double negative charge; V – the cationic/anionic vacancies; Fe and S indices – are ferrous and sulfur position in lattice, respectively:



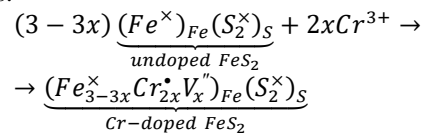
Where x is effective zero charge. The Cr³⁺ doping in FeS₂ can promote generation of cation vacancies due to the follow equation:



The chromium interaction with cation vacancies can be described as:



Taking into account the radii of the metals [$r(Fe^{2+}) = 0.61 \text{ \AA}$, $r(Cr^{3+}) = 0.63 \text{ \AA}$], it is clear that chromium ions can substitute the ferrous ions in their positions:



The formation of chromium cations Cr_{Fe}^* with positive effective charge led's to the simultaneously

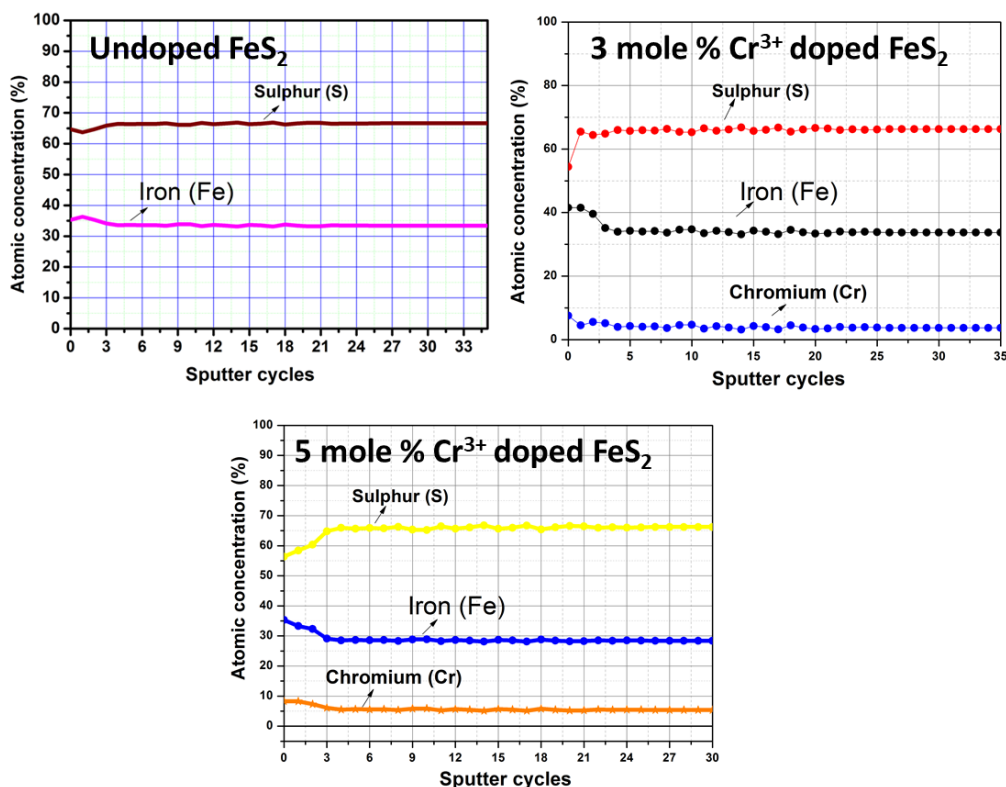
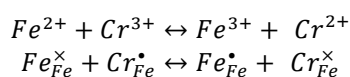


Fig. 9. Auger electron spectroscopy of undoped FeS₂, 3 mole % Cr³⁺ doped FeS₂ and 5 mole % Cr³⁺ doped FeS₂ thin films.

creation of an equivalent amount of negative charged cation vacancies (V_x'')_{Fe}.

In the present system the redox pairs such as Cr³⁺/Cr²⁺ and Fe²⁺/Fe³⁺ that might promote electron transfer process [37-38]. By considering, their standard reduction potentials (E° (Cr³⁺/Cr²⁺) = -0.407 V, E° (Fe²⁺/Fe³⁺) = 0.771 V), it can be concluded that these redox pairs promote electron transfer:



In photocatalytic properties and charge transfer efficiency both are improved by the chromium doping because of the increased of active centers in Cr³⁺ doped FeS₂. This assumption is in good agreement with electrochemical studies discussed in section 3.5 (photocurrent studies) of this article.

2.8. Auger electron spectroscopy (AES) studies

Auger electron spectroscopy was adopted to investigate the surface elemental composition of undoped FeS₂, 3 mole % Cr³⁺ doped FeS₂ and 5 mole % Cr³⁺ doped FeS₂ films and the results are presented in Fig. 9. From figure, the incidence of Fe and S atoms on the surface layer of un doped sample and the presence of Cr³⁺ was confirmed in 3 mole % and 5 mole % samples, with higher content of Cr was observed in latter case.

Conclusion

In this work, Chromium doped iron pyrite thin films were deposited on ITO glass substrates by electrochemical deposition technique. The cubic crystal structure with (200) preferential orientation in FeS₂ and Cr³⁺ doped FeS₂ films was confirmed through XRD. The AFM analysis revealed that the average roughness (R_a) and root-mean square roughness (RMS) of 1 and 5 mole % Cr³⁺ doped FeS₂ films are in the range of 48.5 - 101.67 nm and 46.31 - 128.36 nm. The CV and EIS measurements shown that the 3 mole % Cr³⁺ doped FeS₂ thin films displayed low-charge transfer resistance and enhanced electrocatalytic activity for the reduction of I₃⁻ to I⁻ ions compared to other Cr³⁺ doped FeS₂ films. Among all samples, the 3 mole % Cr³⁺ doped FeS₂ thin film presented a more synergistic effect for the reduction of I₃⁻, which may be due to presence of increased active sites and fast reaction kinetics for the I/I₃⁻ redox reaction. From the results, it can be inferred that Cr³⁺ (3 mole %) doped FeS₂ thin films are the promising candidates of highly efficient and replaceable material for electrocatalytic activity and photo-electrochemical performance.

Acknowledgements

One of the authors (Dr. P. Prabukanthan) wishes to acknowledge University Grant Commission (UGC), India, for the financial assistance through major research project (MRP) scheme [File No.43-399/2014(SR)].

P. Prabukanthan – M.Sc., M.Phil., Ph.D., Assistant Professor;	T. Tatarchuk – M.Sc., Ph.D., Associated Professor;
M. Sreedhar – M.Sc., M.Phil., Research Scholar;	K. Dinakaran – M.Sc., B.Ed., Ph.D., Professor;
G. Harichandran – M.Sc., Ph.D., Associated Professor;	S. Uthayakumar – M.Sc., M.Phil., Ph.D., Senior Research Officer;
	A. Younis – M.Sc., Ph.D., Assistant Professor.

- [1] Y. Liang, P. Bai, J. Zhou, T. Wang, B. Luo and S. Zheng, *Cryst. Eng. Comm.* 18, 6262 (2016); <https://doi.org/10.1039/C6CE01203E>.
- [2] A. Ennaoui, S. Fiechter, C. Pettenkofer, N. Alonso-Vante, K. Buker, M. Bronold, C. Hopfner and H. Tributsch, *Sol. Energy Mater. Sol. Cells.* 29, 289 (1993); [https://doi.org/10.1016/0927-0248\(93\)90095-K](https://doi.org/10.1016/0927-0248(93)90095-K).
- [3] A. Kirkemide, P. Gingrich, M. Gong, H. Cui and S. Re, *Nanotechnology* 25, 205603 (2014); <https://doi.org/10.1088/0957-4484/25/20/205603>.
- [4] P. Prabukanthan, S. Thamaraiselvi and G. Harichandran, *J. Mater. Sci. Mater. Electron* 29, 11951 (2018); <https://doi.org/10.1007/s10854-018-9297-4>.
- [5] A. Pascual, S. Yoda, M. Barawi, J.M. Clamagirand, J.R. Ares, I.J. Ferrer and C. Sanchez, *J. Phys. Chem. C* 118, 26440 (2014); <https://doi.org/10.1021/jp505303d>.
- [6] S. Shukla, W. Ager Joel, Q. Xiong, and T. Sritharan, *Energy Technol.* 6, 8 (2018); <https://doi.org/10.1002/ente.201700638>.
- [7] F. Liu, J. Zhu, L. Hu, B. Zhang, J. Yao, M.K. Nazeeruddin, M. Gratzel and S. Dai, *J. Mater. Chem. A* 3, 6315 (2015) <https://doi.org/10.1039/C5TA00028A>.
- [8] M.R. Gao, Y.F. Xu, J. Jiang and S.H. Yu, *Chem. Soc. Rev.* 42, 2986 (2013); <https://doi.org/10.1039/C2CS35310E>.
- [9] D. Liang, R. Ma, S. Jiao, G. Pang and S. Feng, *Nanoscale* 4, 6265 (2012); <https://doi.org/10.1039/C2NR31193C>.
- [10] J. Jiang, L. Zhu, H. Chen, Y. Sun, H. Lin, S. Han, *J. Alloys Compds.* 775, 1293 (2019); <https://doi.org/10.1039/C3RA46248J>.
- [11] Sadia Khalid, M. Azad Malik, J. Lewis David, P. Kevin, E. Ahmed, Y. Khan, Paul O'Brien, *J Mater Chem C* 3, 12068 (2015); <https://doi.org/10.1039/C5TC03275J>.
- [12] P. Prabukanthan, S. Thamaraiselvi and G. Harichandran, *J. Electrochem. Soc.* 164, 581 (2017); <https://doi.org/10.1149/2.09917.09jes>.
- [13] G. Chatzitheodrou, S. Fiechter, M. Kunst, W. Jaegermann and H. Tributsch, *Mater. Res. Bull.* 21, 1481 (1986); [https://doi.org/10.1016/0025-5408\(86\)90088-7](https://doi.org/10.1016/0025-5408(86)90088-7).
- [14] B. Meester, L. Reijnen, A. Goossens and J. Schoonman, *Chem. Vap. Deposition* 3, 121 (2000); [https://doi.org/10.1002/\(SICI\)1521-3862\(200006\)6](https://doi.org/10.1002/(SICI)1521-3862(200006)6).
- [15] E.J. Kim and B. Batchelor, *Mater. Res. Bull.* 44, 1553 (2009); <https://doi.org/10.1016/j.materresbull.2009.02.006>.
- [16] D. Wan, Q. He, L. Zhang, Q. Jia, R. Zhang, H. Zhang, B. Wang and L. Wei, *J. Crystal Growth* 268, 222 (2004); <https://doi.org/10.1016/j.jcrysgro.2004.05.014>.
- [17] D. Lichtenberger, K. Ellmer, R. Schieck, S. Fiechter and H. Tributsch, *Thin Solid Films* 246, 6 (1994); [https://doi.org/10.1016/0040-6090\(94\)90723-4](https://doi.org/10.1016/0040-6090(94)90723-4).
- [18] I. Ferrer, F. Cabellero, C. De las Heras and C. Sanchez, *Solid State Commun.* 89, 349 (1994); [https://doi.org/10.1016/0038-1098\(94\)90598-3](https://doi.org/10.1016/0038-1098(94)90598-3).
- [19] S. Lehner, N. Newman, M. Van Schilfgaarde, S. Bandyopadhyay, K. Savage and P. Buseck, *J. Appl. Phys.* 111, 083717 (2012); <https://doi.org/10.1063/1.4706558>.
- [20] J. Jiao, L. Chen, D. Kuang, W. Gao, H. Feng and J. Xia, *RSC Adv.* 1, 255 (2011); <https://doi.org/10.1039/C1RA00066G>.
- [21] W. Ding, X. Wang, H. Peng, Z. Peng and B. Dong, *Mater. Res. Bull.* 48, 4704 (2013); <https://doi.org/10.1016/j.materresbull.2013.08.022>.
- [22] R.J. Soukup, P. Prabukanthan, N.J. Ianno, A. Sarkar, C.A. Kamler, and D.G. Sekora, *J. Vac. Sci. Technol. A* 29, 011001 (2011); <https://doi.org/10.1116/1.3517739>.
- [23] S. Khalid, E. Ahmed, M.A. Malik, David Lewis and S. Abu Bakar, *New J. Chem.* 39, 1013 (2015); <https://doi.org/10.1039/C4NJ01461H>.
- [24] S.S. Starchikov, I.S. Lyubutin, Chun-Rong Lin, Yaw-Teng Tseng, K.O. Funtov, Yu Ogarkova, T.V. Dmitrieva and A.G. Ivanova, *Phys. Chem. Chem. Phys.* 17, 15829 (2015); <https://doi.org/10.1039/C5CP01846C>.
- [25] A. Akbar, Muntaha Niaz, Saira Riaz and S. Naseem, *Materials Today: Proc.* 2, 5679 (2015); <https://doi.org/10.1016/j.matpr.2015.11.109>.
- [26] A.E. Kandjanian, M.F. Tabrizia, O.M. Moradia, H.R. Mehra, S. Ahmadi Kandjanib, and M.R. Vaezia, *J. Alloy Com.* 509, 785 (2011); <https://doi.org/10.1016/j.jallcom.2011.01.133>.
- [27] N. Barreau, J. C. Bernede, S. Marsillac and A. Mokrani, *J. Crystal Growth* 235, 439 (2002); [https://doi.org/10.1016/S0022-0248\(01\)02040-1](https://doi.org/10.1016/S0022-0248(01)02040-1).

- [28] P. Prabukanthan, R.J. Soukup, N.J. Ianno, A. Sarkar, C.A. Kamler, E.L. Extrom, J. Olejnicek and S.A. Darveau, Chemical bath deposition (CBD) of iron sulfide thin films for photovoltaic applications, crystallographic and optical properties, Proceedings of the 35th Photovoltaics specialists Conference, Institute of Electrical and electronics Engineers (IEEE) 002965 (2010); <https://doi.org/10.1109/PVSC.2010.5614465>.
- [29] P. Prabukanthan, M. Sreedhar, S. Thamaraiselvi, G. Harichandran, P. Seenuvasakumaran, Marlia Hanafiah and Carlos Fernandez, J. Mater. Sci.: Mater. Electron. 32, 6331 (2021); Photoelectrochemical applications of electrochemical deposition of Ni²⁺-doped FeS₂ thin films, <https://doi.org/10.1007/s10854-018-00599-w>.
- [30] J.H. Kim, H. Kim, D. Kim, S.G. Yoon and W.K. Choo, Solid State Comm. 131, 677 (2004); <https://doi.org/10.1016/j.ssc.2004.06.033>.
- [31] P. Prabukanthan and R. Dhanasekaran, J. Physics D: Appl. Phys. 41, 115102 (2008); <https://doi.org/10.1088/0022-3727/41/11/115102>.
- [32] R. Chand, E. Obuchi, K. Katoh, H. N. Luite and K. Nakano, J. Environ. Sci. 25, 1419 (2013); [https://doi.org/10.1016/S1001-0742\(12\)60211-3](https://doi.org/10.1016/S1001-0742(12)60211-3).
- [33] P. Prabukanthan, S. Thamaraiselvi, G. Harichandran and J. Theerthagiri, J. Mater. Sci.: Mater. Electron. 30, 3268 (2019); <https://doi.org/10.1007/s10854-018-00599>.
- [34] P. Prabukanthan, R. Lakshmi, G. Harichandran and T. Tatarchuk, New J. Chem. 42, 11642 (2018); <https://doi.org/10.1039/c8nj01056k>.
- [35] T. Rajesh Kumar, P. Prabukanthan, G. Harichandran, J. Theerthagiri, A. MeeraMoydeen, G. Durai, P. Kuppusami and Tetiana Tatarchuk, J. Mat. Sci.: Mat. Electro. 29, 5638 (2018); <https://doi.org/10.1007/s10854-018-8533-2>.
- [36] T. RajeshKumar, P. Prabukanthan, G. Harichandran, J. Theerthagiri, Tetiana Tatarchuk, T. Maiyalagan, J. Solid State Electrochem. 22, 1197 (2018); <https://doi.org/10.1007/s10008-017-3865-z>.
- [37] Xiaoliang Liang, Yuanhong Zhong, Hongping He, Peng Yuan, Jianxi Zhu, Sanyuan Zhu, Zheng Jiang, Chem. Eng. J. 191, 177 (2012); <https://doi.org/10.1016/j.cej.2012.03.001>.
- [38] Rui Ribeiro, M. T. Adrián, Silva, José Figueiredo, Joaquim Faria and Helder Gomes, Catal. Today. 296, 66 (2017); <https://doi.org/10.1016/j.cattod.2017.06.023>.

П. Прабукантан¹, М. Свідхар¹, Г. Харічандран², Т. Татарчук³, К. Дінакаран⁴,
С. Утаякумар^{5,6}, А. Йоуніс⁷

Фізико-хімічні та електрокаталітичні характеристики тонких плівок піриту заліза, легованого хромом

¹Урядовий коледж мистецтв Мутхурангама, Веллор, Індія, pprabukanthan76@hotmail.com

²Університет Мадраса, Кампус Гінді, Ченнаї, Індія

³Прикарпатський національний університет імені Василя Стефаника, Івано-Франківськ, 76018, Україна

⁴Університет Тіруваллувар, Веллор, Індія

⁵Лондонський Королівський університет Холловей, Егам, TW20 0EX, Великобританія

⁶ISIS, STFC, Лабораторія Резерфорда Еплтона, Дідкот, Оксфордшир OX11 0QX, Великобританія

⁷Кафедра фізики, Коледж наук, Університет Бахрейну, кампус Сахір, Королівство Бахрейн

Тонкі плівки піриту заліза (FeS₂), легованого хромом (Cr³⁺), наносили на підкладку ІТО за допомогою процесу електрохімічного осадження. Досліджено вплив вмісту хрому на структурну, оптичну, електричну, морфологічну та електрокаталітичну поведінку тонких плівок піриту. Рентгенодифракційні дослідження підтвердили формування кубічної кристалічної структури нанесених тонких плівок. Результати атомно-силової мікроскопії вказують, що легування Cr³⁺ має сильний вплив на кристалічність, шорсткість поверхні та розмір зерен напилених тонких плівок. Крім того, у тонких плівках FeS₂, легованих Cr³⁺, спостерігалосся зменшення забороненої зони. Опір між поверхневим зарядом виготовлених тонких плівок досліджено за допомогою електрохімічної імпедансної спектроскопії. Тонкі плівки FeS₂, леговані 3 моль % Cr³⁺, показали чудову провідність із низьким опором передачі заряду 49 Ом. Також досліджено електрокаталітичні властивості отриманих тонких плівок піриту. Виявлено, що тонкі плівки, леговані хромом, демонструють кращі характеристики. Для дослідження характеристик дефектів у виготовлених тонких плівках вибрано антиструктурне моделювання, і встановлено, що заміщення Cr³⁺ може утворювати катіонні (Fe²⁺) вакансії, які можуть відповідати за посилення фотохімічної та електрохімічної активності у тонких плівках FeS₂, легованих Cr.

Ключові слова: електрохімічне осадження; напівпровідникові тонкі плівки; пірит; імпедансна спектроскопія; електрокаталітична активність; аналіз поверхні.